

Strengthened Partial-Ordering Based ILP Models for the Vertex Coloring Problem

Adalat Jabrayilov ✉ 

Institute of Computer Science, University of Bonn, Bonn, Germany

Petra Mutzel ✉ 

Institute of Computer Science, University of Bonn, Bonn, Germany

Abstract

The vertex coloring problem asks for the minimum number of colors that can be assigned to the vertices of a given graph such that each two adjacent vertices get different colors. For this NP-hard problem, a variety of integer linear programming (ILP) models have been suggested. Among them, the *assignment* based and the *partial-ordering* based ILP models are attractive due to their simplicity and easy extendability. Moreover, on sparse graphs, both models turned out to be among the strongest exact approaches for solving the vertex coloring problem. In this work, we suggest additional strengthening constraints for the *partial-ordering* based ILP model, and show that they lead to improved lower bounds of the corresponding LP relaxation. Our computational experiments confirm that the new constraints are also leading to practical improvements. In particular, we are able to find the optimal solution of a previously open instance from the DIMACS benchmark set for vertex coloring problems.

2012 ACM Subject Classification Mathematics of computing → Graph theory; Mathematics of computing → Mathematical optimization

Keywords and phrases Graph theory, integer linear programming, polyhedral theory, vertex coloring problem

Digital Object Identifier 10.4230/LIPIcs.CVIT.2016.23

Funding This work is funded by the DFG under Germany's Excellence Strategy EXC-2047/1 – 390685813.

1 Introduction

Given a graph $G = (V, E)$, the vertex coloring problem searches for the assignment of colors to the vertices, such that no two adjacent vertices get the same color and the number of colors is minimized. The minimum number of colors needed is called the *chromatic number* of G . Finding the chromatic number is known to be NP-hard [12]. Due to the wide range of applications like register allocation, scheduling, frequency assignment and timetabling problems, there is a vast amount of literature on this problem. For surveys, see for example [17, 20, 21, 23].

The exact algorithms for the VCP can be divided into dynamic programming approaches [3, 7, 11, 19], branch-and-bound based enumeration [1, 2, 9, 24, 31, 32, 35], and integer linear programming approaches [5, 6, 15, 18, 22, 25, 26, 27]. The dynamic programming algorithms require exponential space of $O(2^{|V|})$ and are of theoretical interest only. In contrast, the branch-and-bound algorithms require only polynomial space and are applicable to graphs with up to 80 vertices [31]. However, the most efficient algorithms for large instances are ILP-based algorithms. State-of-the-art ILP models are the *assignment* based model [26, 27], the *partial-ordering* based model [18], the *representatives* model [4, 5, 6], the set covering and set partitioning models [25, 22, 15], and the *ordered binary decision diagrams (OBDD)* based model [34].



© Adalat Jabrayilov and Petra Mutzel;
licensed under Creative Commons License CC-BY 4.0

42nd Conference on Very Important Topics (CVIT 2016).

Editors: John Q. Open and Joan R. Access; Article No. 23; pp. 23:1–23:19

Leibniz International Proceedings in Informatics



LIPICs Schloss Dagstuhl – Leibniz-Zentrum für Informatik, Dagstuhl Publishing, Germany

These models can be divided into two groups: *explicit coloring models* and *independent set based models*. *Explicit coloring models* directly create a coloring function $c: V \rightarrow \mathbb{N}$. Prominent members of this class are the *assignment* and the *partial-ordering based models* [26, 18]. Both models have $O(|V|H)$ variables and $O(|E|H)$ constraints, where H is an upper bound for the chromatic number of the graph [26, 18]. If the graph is sparse, then H is expected to be a small number. Hence these two models are best suited for sparse graphs.

Independent set based models partition the vertex set of the given graph so that every part induces an independent set and thus corresponds to a color class. The models include the representatives model [4], the set covering and set partitioning models [25, 22, 15], and the *reduced ordered binary decision diagram* approach. The representatives model [4] has $O(|V| + |\bar{E}|)$ variables and $O(|V| + |V||E|)$ constraints, where \bar{E} is the set of edges of the complement graph. As the density increases, the number $|\bar{E}|$ and hence the number of variables decreases. Obviously, this model is particularly suitable for dense graphs, which was also confirmed in practical experiments (see, e.g., [18]). The set covering and set partitioning formulations involve a variable for each independent set and are best suited for dense graphs. Unlike the first three models, these models have an exponential number of variables and therefore need to be solved with sophisticated branch-and-price algorithms. In contrast to the previous models, the decision diagrams approach first transforms the vertex coloring problem for graph G into a reduced ordered binary decision diagram (OBDD), and then computes a constrained flow on this OBDD by solving a network flow based ILP formulation. The reduced OBDD is a *directed acyclic graph (DAG)* with exactly one source s and one sink t and contains a directed (s, t) -path for each independent set in G . This model is also particularly suitable for dense graphs, since the number of independent sets, and thus the number of (s, t) -paths in the OBDD, becomes smaller with increasing density.

A typical solution process of such an ILP model first solves the LP relaxation, i.e., the corresponding linear program (LP) in which the integer requirements are dropped. This leads to a first lower bound for the optimal solution value of the integer linear program. If the LP values of the variables are integral, we have found an integer solution which coincides with the lower bound. Otherwise, we start a branch-and-bound possibly combined with a cutting plane approach and/or a column generation (pricing) approach. In the course of the branch-and-bound, the gap between the lower and the upper bounds decreases. If the lower and upper bounds coincide, we have found an optimal solution for our ILP.

Theoretical and practical analyses have shown that the lower bounds achieved by the assignment and the partial-ordering based approaches are weaker (i.e., lower) than those of the models based on independent sets such as the representatives model, the set-covering model, and the OBDD based model. However, for sparse graphs G , the chromatic number $\chi(G)$ and also the gap between the lower bound and $\chi(G)$ is generally small. This observation jointly with the fact that the number of variables and constraints of the assignment and partial-ordering ILP models is much smaller than those of the independent set based models, justifies the efficiency of the aforementioned models on sparse graphs.

Our contribution. In this paper, we consider the partial-ordering based ILP model. This has recently attracted interest by researchers who applied the partial-ordering model to problems related to the VCP such as the *Filter Partitioning Minimization Problem* [30], the *Multi-Page Labeling Problem* [13], and the *Equitable Chromatic Number Problem* [28], in which the task is to color the vertices so that adjacent vertices get different colors and the size of the color classes is approximately the same.

■ We propose to add some *strengthening constraints* to the partial-ordering model and

- prove that their addition improves the lower bound of the corresponding LP relaxation.
- Our polyhedral investigations show that the strengthened partial-ordering model leads to stronger lower bounds of the LP relaxations in comparison to the assignment model.
 - We present computational experiments that show that our strengthened partial-ordering model also leads to practical improvements. The computational results also include an open DIMACS [33] instance, which is solved for the first time (up to our knowledge).
 - Our experimental comparison with state-of-the-art approaches on the DIMACS benchmark set shows that, as expected, the assignment and the partial-ordering based approaches outperform the set-covering and OBDD based models on sparse graphs.

Outline. Section 2 provides the basic notations. (Section 2). We describe the assignment and the partial-ordering based ILP models as well as their extensions in Section 3. The theoretical analysis of the corresponding polytopes and lower bounds is given in Section 4. Section 5 describes and discusses the computational experiments.

2 Notations

We denote the set $\{1, \dots, k\}$ by $[k]$. For a graph $G = (V, E)$, we denote its vertex set by $V(G)$ and its edge set by $E(G)$. For clarity, we may write the edge $e = \{u, v\}$ for $u, v \in V$ as $e = uv$. By $N(v) := \{u \in V \mid uv \in E\}$ we denote the set of neighbors of v . A *walk* W in a graph is a sequence $W = v_0, e_1, v_1, \dots, v_{k-1}, e_k, v_k$ of not necessarily distinct vertices and edges, such that $e_i = v_{i-1}v_i$ for $i \in [k]$. A walk is a (*simple*) *path* if all its vertices are distinct. We may describe W as the sequence of its vertices v_0, \dots, v_k or edges e_1, \dots, e_k . A walk W is called *cycle* if $v_0 = v_k$. A cycle $C := e_1, \dots, e_k$ is called *odd* if k is odd.

3 Assignment and partial-ordering based models

In the following we assume that the graph $G = (V, E)$ is connected and has at least one vertex. Obviously, the problem can be solved separately on each connected component.

3.1 Assignment-based ILP models

The idea of the assignment based model for the vertex coloring problem is very natural: namely, the model assigns color i to vertex $v \in V$. For this, it introduces *assignment variables* x_{vi} for each vertex $v \in V$ and color $i \in [H]$, with $x_{vi} = 1$ if vertex v is assigned to color i and $x_{vi} = 0$ otherwise. H is an upper bound of the chromatic number of G (e.g., the solution value of some heuristic for the problem) and is bounded by $|V|$. For modelling the objective function, additional binary variables w_i for $i \in [H]$ are needed, which get value 1 if and only if color i is used in the coloring. The model is given by:

$$\begin{aligned}
 \text{ASS :} \quad & \min \sum_{1 \leq i \leq H} w_i \\
 & \text{subject to} \\
 & \sum_{i=1}^H x_{vi} = 1 \quad \text{for all } v \in V \quad (1) \\
 & x_{ui} + x_{vi} \leq w_i \quad \text{for all } uv \in E, i = 1, \dots, H \quad (2) \\
 & w_i \leq \sum_{v \in V} x_{vi} \quad i = 1, \dots, H \quad (3) \\
 & w_i \leq w_{i-1} \quad i = 2, \dots, H \quad (4) \\
 & x_{vi}, w_i \in \{0, 1\} \quad \text{for all } v \in V, i = 1, \dots, H \quad (5)
 \end{aligned}$$

The objective function minimizes the number of used colors. Equation (1) ensures that each vertex receives exactly one color. For each edge $uv \in E$ there is a set of constraints (2) making sure that adjacent vertices receive different colors. These constraints at the same time ensure that a color i can be assigned only to one of the vertices if the variable w_i is set to 1. The assignment model with constraints (1), (2), and (5) has the advantage that it is simple and easy to use. It can be easily extended to generalizations and/or restricted variants of the graph coloring problem. A main drawback of the model is that there are $\binom{H}{\chi}$ possibilities to select χ from H colors [23]. This results in many optimal solutions that are symmetric to each other, which is a big problem for branch-and-bound approaches. In order to overcome this symmetry, Mendez-Diaz and Zabala [26, 27] have suggested to add the constraints (3) and (4).

3.2 Partial-ordering based ILP models

Instead of directly assigning a color to the vertices, the partial-ordering based model determines the partial order $(V \cup [H], \prec)$ of the union of the vertex set V and the set $[H]$ of ordered colors, where H is an upper bound for the chromatic number $\chi(G)$. This model has two binary variables $l_{v,i}$ and $g_{i,v}$ for each vertex $v \in V$ and each color $i \in [H]$, where $l_{v,i} = 1$ iff $v \prec i$ (i.e., the color of v is smaller than i), and $g_{i,v} = 1$ iff $i \prec v$ (the color of v is larger than i). These variables have the following connection with the assignment variables. Vertex v has color i (i.e., $x_{v,i} = 1$) if and only if i and v are not ordered in \prec , i.e., we have $v \not\prec i$ and $i \not\prec v$ ($l_{v,i} = g_{i,v} = 0$), thus we have:

$$x_{v,i} = 1 - (l_{v,i} + g_{i,v}) \quad \text{for all } v \in V, i = 1, \dots, H. \quad (6)$$

The POP model [18] has the following form, where q is an arbitrary vertex chosen from V :

$$\begin{aligned} \text{POP :} \quad & \min 1 + \sum_{1 \leq i \leq H} g_{i,q} \\ & \text{subject to} \end{aligned}$$

$$l_{v,1} = g_{H,v} = 0 \quad \text{for all } v \in V \quad (7)$$

$$g_{i-1,v} - g_{i,v} \geq 0 \quad \text{for all } v \in V, i = 2, \dots, H \quad (8)$$

$$g_{i-1,v} + l_{v,i} = 1 \quad \text{for all } v \in V, i = 2, \dots, H \quad (9)$$

$$(g_{i,u} + l_{u,i}) + (g_{i,v} + l_{v,i}) \geq 1 \quad \text{for all } uv \in E, i = 1, \dots, H \quad (10)$$

$$g_{i,q} - g_{i,v} \geq 0 \quad \text{for all } v \in V, i = 1, \dots, H \quad (11)$$

$$g_{i,v}, l_{v,i} \in \{0, 1\} \quad \text{for all } v \in V, i = 1, \dots, H. \quad (12)$$

Constraints (7)–(9) ensure that each vertex receives exactly one color. Every adjacent pair of vertices must receive different colors. This is guaranteed by constraints (10). Constraints (11) enforce that there is no vertex $v \in V$ with $q \prec v$ in the partial order \prec , i.e., the chosen vertex q has the largest used color.

3.2.1 Strengthening the POP model

Here we provide additional constraints that strengthen the LP relaxations of the models, i.e., lead to improved lower bounds.

Using equations (7) and (9), one can eliminate all the l -variables [18]. Setting these equations to (10) yields:

$$g_{1,u} + g_{1,v} \geq 1 \quad \text{for all } uv \in E, \quad (13)$$

$$(g_{i-1,u} - g_{i,u}) + (g_{i-1,v} - g_{i,v}) \leq 1 \quad \text{for all } uv \in E, i = 2, \dots, H. \quad (14)$$

In the following, we show how to strengthen constraints (13) and (14). Similar to the assignment model's constraints (2) we can tighten the right hand side of (13) and (14) by replacing the constant by a variable as follows. Constraint (13) forces either $g_{1,u} = 1$ or $g_{1,v} = 1$, and from (11) we get $g_{1,q} = 1$. Thus we can replace (13) by

$$g_{1,u} + g_{1,v} \geq 2 - g_{1,q} \quad \text{for all } uv \in E. \quad (15)$$

If the left hand side of (14) is equal to 1, then either $g_{i-1,u} = 1$ or $g_{i-1,v} = 1$. Then $g_{i-1,q} = 1$ by (11). Thus we can tighten (14) as follows:

$$(g_{i-1,u} - g_{i,u}) + (g_{i-1,v} - g_{i,v}) \leq g_{i-1,q} \quad \text{for all } uv \in E, i = 2, \dots, H. \quad (16)$$

We denote the tightened program by POP1:

$$\begin{aligned} \text{POP1 :} \quad & \min 1 + \sum_{1 \leq i \leq H} g_{i,q} \\ & \text{subject to} \\ & g_{H,v} = 0 \quad \text{for all } v \in V \quad (17) \\ & g_{i-1,v} - g_{i,v} \geq 0 \quad \text{for all } v \in V, i = 2, \dots, H \quad (18) \\ & g_{1,u} + g_{1,v} \geq 2 - g_{1,q} \quad \text{for all } uv \in E \quad (19) \\ & (g_{i-1,u} - g_{i,u}) + (g_{i-1,v} - g_{i,v}) \leq g_{i-1,q} \quad \text{for all } uv \in E, i = 2, \dots, H \quad (20) \\ & g_{i,q} - g_{i,v} \geq 0 \quad \text{for all } v \in V, i = 1, \dots, H \quad (21) \\ & g_{i,v} \in \{0, 1\} \quad \text{for all } v \in V, i = 1, \dots, H. \quad (22) \end{aligned}$$

Our second model POP2 further strengthens the POP1 model. For all $v \in N(q)$, $i \prec v$ ($g_{i,v} = 1$) implies $i + 1 \prec q$ ($g_{i+1,q} = 1$). This statement can be formulated as follows:

$$g_{i+1,q} - g_{i,v} \geq 0 \quad \text{for all } v \in N(q), i = 1, \dots, H - 1. \quad (23)$$

We extend POP1 by the constraints (23) and denote the resulted ILP by POP2.

3.3 A hybrid partial-ordering based model for VCP

The second model in [18] is a hybrid of the assignment and the partial-ordering based models and uses the observation that with growing density the POP constraint matrix contains more non-zero elements than that of ASS, since the POP constraints (10) contain twice as many non-zero coefficients as the corresponding ASS constraints (2). Hence one can substitute (10) by equalities (6) and the following constraints:

$$x_{u,i} + x_{v,i} \leq 1 \quad \text{for all } uv \in E, i = 1, \dots, H. \quad (24)$$

3.3.1 Strengthening the hybrid POP model

We can strengthen the hybrid model analogous to the pure model POP. If the graph has an edge, we have $g_{1,q} = 1$. Hence, in case $i = 1$, we can replace (24) by

$$x_{u,1} + x_{v,1} \leq g_{1,q} \quad \text{for all } uv \in E. \quad (25)$$

If the color of a vertex v is i (i.e., $x_{v,i} = 1$) for $i \geq 2$, then its color is larger than $i - 1$ (i.e., $g_{i-1,v} = 1$). It follows that in the case $x_{u,i} = 1$ or $x_{v,i} = 1$, we have $g_{i-1,u} = 1$ or $g_{i-1,v} = 1$, and thus $g_{i-1,q} = 1$ by (11). Therefore, we can replace (24) by

$$x_{u,i} + x_{v,i} \leq g_{i-1,q} \quad \text{for all } uv \in E, i = 2, \dots, H. \quad (26)$$

Using equations (7) and (9), we eliminate all the l -variables. This elimination transforms the equalities (6) into the following form:

$$\begin{aligned} x_{v,1} &= 1 - g_{1,v} && \text{for all } v \in V, \\ x_{v,i} &= g_{i-1,v} - g_{i,v} && \text{for all } v \in V, i = 2, \dots, H. \end{aligned}$$

Notice that these constraints jointly with constraints $x_{v,i} \in [0, 1]$ imply the inequalities (8). Therefore, constraints (8) are redundant in the hybrid model. We denote the tightened hybrid partial-ordering program by POPH1.

$$\begin{aligned} \text{POPH1 : } \min \quad & 1 + \sum_{1 \leq i \leq H} g_{i,q} \\ \text{subject to} \quad & \\ & g_{H,v} = 0 && \text{for all } v \in V && (27) \\ & x_{v,1} = 1 - g_{1,v} && \text{for all } v \in V && (28) \\ & x_{v,i} = g_{i-1,v} - g_{i,v} && \text{for all } v \in V, i = 2, \dots, H && (29) \\ & x_{u,1} + x_{v,1} \leq g_{1,q} && \text{for all } uv \in E && (30) \\ & x_{u,i} + x_{v,i} \leq g_{i-1,q} && \text{for all } uv \in E, i = 2, \dots, H && (31) \\ & g_{i,q} - g_{i,v} \geq 0 && \text{for all } v \in V, i = 1, \dots, H && (32) \\ & x_{v,i}, g_{i,v} \in \{0, 1\} && \text{for all } v \in V, i = 1, \dots, H. && (33) \end{aligned}$$

Similar to the pure pop model POP2, we also generate a hybrid model POPH2, which extends POPH1 by the constraints (23).

► **Remark 1 (non-zero coefficients).** Simply counting the non-zero coefficients in the constraint matrix of the pure and the hybrid POP models gives $(6|V| + 5|E|) \cdot H - |V| - 2|E|$ and $(9|V| + 3|E|) \cdot H$, respectively. This means that the constraint matrix of the hybrid model becomes sparser than that of the pure model with increasing $|E|$.

4 Polyhedral Results

In this section we show the polyhedral advantages of the partial-ordering based models over the assignment model for the VCP. In particular, we study the LP relaxations of the models POP1 and POP2. By solving such an LP relaxation, we obtain a fractional solution. The solution value of these relaxations is also called the *dual bound* to the optimal solution value of the original ILP model.

We first consider the dual bounds of the partial-ordering based models POP1 and POP2 and show that they are larger than two for all connected graphs with $\chi(G) \geq 3$.

4.1 Dual Bound of POP1

► **Lemma 2.** *Let $C := q, v_1, v_2, \dots, v_{2k}, q$ with $k \geq 1$ be an odd cycle in G , where q is the chosen vertex in the partial-ordering based models. Then:*

$$\nu(\text{POP1}) \geq \begin{cases} 2 + \frac{1}{3} & k = 1 \\ 2 + \frac{1}{k+1} & k \geq 2. \end{cases}$$

Proof. Adding (20) for an edge uv and each $i = 2, \dots, H$ gives:

$$\sum_{i=1}^{H-1} g_{i,q} \geq g_{1,u} + g_{1,v} - g_{H,u} - g_{H,v} \quad \text{for all } uv \in E.$$

As $g_{H,q} = g_{H,u} = g_{H,v} = 0$ by (17), we can rewrite these inequalities as follows:

$$\sum_{i=1}^H g_{i,q} \geq g_{1,u} + g_{1,v} \quad \text{for all } uv \in E. \quad (34)$$

Case $k = 1$: C has exactly three vertices, i.e., $C := q, v_1, v_2, q$. Adding the inequalities (34) for edges $qv_1, qv_2 \in E$ gives:

$$2 \sum_{i=1}^H g_{i,q} \geq 2g_{1,q} + g_{1,v_1} + g_{1,v_2}. \quad (35)$$

The sum of the constraints

$$\begin{aligned} \sum_{i=1}^H g_{i,q} &\geq g_{1,q} + \frac{1}{2}g_{1,v_1} + \frac{1}{2}g_{1,v_2} && // \frac{1}{2} \times (35) \\ 0 &\geq \frac{1}{2}(2 - g_{1,q} - g_{1,v_1} - g_{1,v_2}) && // \frac{1}{2} \times (19) \text{ for edge } v_1v_2 \in E \\ 0 &\geq \frac{1}{6}(2 - g_{1,q} - g_{1,q} - g_{1,v_1}) && // \frac{1}{6} \times (19) \text{ for edge } qv_1 \in E \\ 0 &\geq \frac{1}{6}(-g_{1,q} + g_{1,v_1}) && // \frac{1}{6} \times (21) \text{ for } v_1 \in V \end{aligned}$$

imply $\sum_{i=1}^H g_{i,q} \geq 1\frac{1}{3}$. It follows:

$$\nu(\text{POP1}) = 1 + \sum_{i=1}^H g_{i,q} \geq 2\frac{1}{3}.$$

Case $k \geq 2$: Adding (19) for edges $v_{2j-1}v_{2j}$ with $j = 1, \dots, k$ yields:

$$\sum_{j=1}^k (g_{1,v_{2j-1}} + g_{1,v_{2j}}) \geq k(2 - g_{1,q}). \quad (36)$$

Adding (34) for each edge $v_{2j}v_{2j+1}$ with $j = 1, \dots, k-1$ yields:

$$\sum_{j=1}^{k-1} \sum_{i=1}^H g_{i,q} \geq \sum_{j=1}^{k-1} (g_{1,v_{2j}} + g_{1,v_{2j+1}}). \quad (37)$$

Adding (36) and (37) leads to:

$$\begin{aligned} \sum_{j=1}^{k-1} \sum_{i=1}^H g_{i,q} &\geq \sum_{j=1}^{k-1} (g_{1,v_{2j}} + g_{1,v_{2j+1}}) - \sum_{j=1}^k (g_{1,v_{2j-1}} + g_{1,v_{2j}}) + k(2 - g_{1,q}) \\ &= k(2 - g_{1,q}) - g_{1,v_1} - g_{1,v_{2k}}. \end{aligned} \quad (38)$$

The sum of the constraints

$$\begin{aligned} \sum_{j=1}^{k-1} \sum_{i=1}^H g_{i,q} &\geq k(2 - g_{1,q}) - g_{1,v_1} - g_{1,v_{2k}} && // (38) \\ \sum_{i=1}^H g_{i,q} &\geq g_{1,q} + g_{1,v_1} && // (34) \text{ for edge } qv_1 \in E \\ \sum_{i=1}^H g_{i,q} &\geq g_{1,q} + g_{1,v_{2k}} && // (34) \text{ for edge } qv_{2k} \in E \end{aligned}$$

gives:

$$\begin{aligned} (k+1) \sum_{i=1}^H g_{i,q} &\geq k(2 - g_{1,q}) + 2g_{1,q} \geq 2k - g_{1,q}(k-2) \\ &\geq 2k - (k-2) && // \quad g_{1,q} \leq 1 \\ &= k+2. \end{aligned}$$

It follows $\sum_{i=1}^H g_{i,q} \geq \frac{k+2}{k+1}$. Thus we have:

$$\nu(\text{POP1}) = 1 + \sum_{i=1}^H g_{i,q} \geq 1 + \frac{k+2}{k+1} = 2 + \frac{1}{k+1}.$$

► **Theorem 3.** *Let G be a graph with $\chi(G) > 2$. Then the improved model POP1 satisfies:*

$$\nu(\text{POP1}) \geq 2 + \frac{1}{|V|} > 2.$$

Proof. From $\chi(G) > 2$ it follows that G contains an odd cycle C with $2k + 1$ vertices for some $k \geq 1$. Since G is connected, there is a shortest simple path P that starts at q and ends at a vertex w of C such that $V(P) \cap V(C) = \{w\}$. Then the path q, \dots, w , the cycle C , and the path w, \dots, q build an odd cycle with at most

$$(|V| - 2k - 1) + (2k + 1) + (|V| - 2k - 1) = 2(|V| - k - 1) + 1$$

vertices. Let $k' := (|V| - k - 1)$. By Lemma 4 we have:

$$\nu(\text{POP1}) \geq 2 + \frac{1}{k' + 2} = 2 + \frac{1}{(|V| - k - 1) + 2} = 2 + \frac{1}{|V| - k + 1} \geq 2 + \frac{1}{|V|},$$

where the last inequality follows from $k \geq 1$. ◀

4.2 Dual Bound of POP2

► **Lemma 4.** *Let $C := q, v_1, v_2, \dots, v_{2k}, q$ with $k \geq 1$ be an odd cycle in G , where q is the chosen vertex in the partial-ordering based models. Then:*

$$\nu(\text{POP2}) \geq 2 + \frac{1}{k + 1}.$$

Proof. Recall that POP2 contains all constraints of POP1. Then for $k \geq 2$ we have

$$\nu(\text{POP2}) \geq \nu(\text{POP1}) \geq 2 + \frac{1}{k + 1}.$$

Thus the claim holds for $k \geq 2$. So it is sufficient to consider the case $k = 1$. Then C has three vertices, i.e., $C := q, v_1, v_2, q$. Adding (23) for a neighbor $v \in N(q)$ and each $i = 1, \dots, H - 1$ yields:

$$\sum_{i=2}^H g_{i,q} \geq \sum_{i=1}^{H-1} g_{1,v} \quad \text{for all } v \in N(q).$$

Adding $g_{1,q}$ on both sides of these inequalities yields:

$$\sum_{i=1}^H g_{i,q} \geq g_{1,q} + \sum_{i=1}^{H-1} g_{1,v} \quad \text{for all } v \in N(q). \quad (39)$$

The sum of constraints (39) for both neighbors v_1 and v_2 of q gives:

$$2 \sum_{i=1}^H g_{i,q} \geq 2g_{1,q} + \sum_{i=1}^{H-1} g_{i,v_1} + \sum_{i=1}^{H-1} g_{i,v_2}. \quad (40)$$

The sum of the constraints

$$\begin{aligned} \sum_{i=1}^H g_{i,q} &\geq g_{1,q} + \frac{1}{2} \sum_{i=1}^{H-1} (g_{i,v_1} + g_{i,v_2}) && // \frac{1}{2} \times (40) \\ 0 &\geq 2 - g_{1,q} - g_{1,v_1} - g_{1,v_2} && // 1 \times (19) \text{ for } v_1 v_2 \in E \\ 0 &\geq \frac{1}{2} (-g_{1,q} + (g_{1,v_1} - g_{2,v_1}) + (g_{1,v_2} - g_{2,v_2})) && // \frac{1}{2} \times (20) \text{ for } v_1 v_2 \in E, i = 2 \end{aligned}$$

imply that:

$$\begin{aligned}
 \sum_{i=1}^H g_{i,q} &\geq 2 - \frac{1}{2}g_{1,q} + \frac{1}{2} \sum_{i=3}^{H-1} (g_{i,v_1} + g_{i,v_2}) \\
 &\geq 2 - \frac{1}{2}g_{1,q} \\
 &\geq 2 - \frac{1}{2} \quad // \quad g_{1,q} \leq 1 \\
 &\geq 1\frac{1}{2}.
 \end{aligned}$$

It follows for $k = 1$:

$$\nu(\text{POP2}) = 1 + \sum_{i=1}^H g_{i,q} \geq 2\frac{1}{2} = 2 + \frac{1}{k+1}.$$

◀

4.3 Strength-relationship

Next, we consider the strength-relationship between the assignment and the partial-ordering based models. For polyhedral comparisons we use the term *strength of an LP relaxation* [29]. We denote by $\nu(M)$ the value of the LP relaxation of the ILP M . Let M and M' be two ILPs for a minimization problem P . We say M is stronger than M' , if $\nu(M) \geq \nu(M')$ holds for all instances of P ; M is strictly stronger than M' if M is stronger than M' , but M' is not stronger than M .

► **Lemma 5.** *POP2 is strictly stronger than POP1.*

Proof. The LP relaxation of POP2 is stronger than that of POP1, since the former contains all constraints of the latter. To show that POP1 is not stronger than POP2, it is sufficient to construct a VCP instance with strict inequality $\nu(\text{POP2}) > \nu(\text{POP1})$. Let G be a complete graph with four vertices q, a, b, c , and let $H = 4$. Consider the following feasible solution for the linear program POP1:

$$\begin{aligned}
 (g_{1,q}, g_{2,q}, g_{3,q}, g_{4,q}) &= (4/5, 2/5, 1/5, 0) \\
 (g_{1,v}, g_{2,v}, g_{3,v}, g_{4,v}) &= (3/5, 1/5, 0, 0) \quad \forall v \in V \setminus \{q\}.
 \end{aligned}$$

of value $1 + \sum_{i=1}^H g_{i,q} = 2.4$. It follows that $\nu(\text{POP1}) \leq 2.4$. Since G contains the 3-cycle q, a, b, q we have $\nu(\text{POP2}) \geq 2.5$ by Lemma 4, so $\nu(\text{POP2}) > \nu(\text{POP1})$, as claimed. ◀

► **Lemma 6.** *POP1 is strictly stronger than ASS.*

Proof. We first show that POP1 is stronger than ASS. If G consists of only one vertex, then both models have the same value 1, so suppose G has some edges. The model ASS has the following feasible solution of value 2, valid for any graph [23]:

$$\begin{aligned}
 \text{for all } v \in V : \quad & x_{vi} = \begin{cases} 1/2 & i \in \{1, 2\} \\ 0 & i > 2, \end{cases} \\
 \text{for all } i \in [H] : \quad & w_i = \begin{cases} 1 & i \in \{1, 2\} \\ 0 & i > 2. \end{cases}
 \end{aligned}$$

It follows that the objective value of the assignment model, independent of the graph, is at most 2, i.e., $\nu(\text{ASS}) \leq 2$. On the other hand, if G has an edge, the objective value of POP1

is at least 2, i.e., $\nu(\text{POP1}) \geq 2$. The reason is the following: Adding (19) and (34) for any edge $uv \in E$ gives: $\sum_{i=1}^H g_{i,q} \geq 2 - g_{1,q} \geq 1$. Therefore we have:

$$\nu(\text{POP1}) = 1 + \sum_{i=1}^H g_{i,q} \geq 2.$$

Therefore, for any graph we have $\nu(\text{POP1}) \geq \nu(\text{ASS})$. On the other hand for any graph G with $\chi(G) > 2$, we have $\nu(\text{POP1}) > 2$ by Theorem 3, while $\nu(\text{ASS}) = 2$. ◀

Chosen vertex q in model ASS

In contrast to the assignment model, POP1 has constraints, namely (21), which force the chosen vertex q to take the largest used color. The natural question is how the strength of the assignment model changes if we add similar constraints to it. Equalities (6), (7), and (9) give

$$g_{1,v} = 1 - x_{v,1} \quad \text{for all } v \in V, \quad (41)$$

$$g_{i,v} = g_{i-1,v} - x_{v,i} \quad \text{for all } v \in V, \ i = 2, \dots, H, \quad (42)$$

which jointly imply

$$g_{i,v} = 1 - \sum_{j=1}^i x_{v,j} \quad \text{for all } v \in V, \ i = 1, \dots, H. \quad (43)$$

So we can add (21) to the assignment model as follows:

$$1 - \sum_{j=1}^i x_{q,j} \geq 1 - \sum_{j=1}^i x_{v,j} \quad \text{for all } v \in V \setminus \{q\}, \ i = 1, \dots, H. \quad (44)$$

Notice that these constraints cannot cut off the solution (x, w) shown as an example in the proof of Lemma 6. So, strengthening ASS via (44) does not make it stronger than POP1, since the fact $\nu(\text{ASS}) \leq 2$ remains unchanged.

► **Lemma 7.** *ASS is strictly stronger than POP.*

Proof. In case G consists of only one vertex, both models have the same objective value 1. Therefore we consider the case that G has some edges. The model POP has the solution

$$\text{for all } v \in V : \quad l_{vi} = \begin{cases} 0 & i = 1 \\ 1/2 & i = 2 \\ 1 & i > 2, \end{cases} \quad g_{iv} = \begin{cases} 1/2 & i = 1 \\ 0 & i \geq 2, \end{cases}$$

of objective value $1 + \sum_{i=1}^H g_{i,q} = 1\frac{1}{2}$, independent of the graph, so $\nu(\text{POP}) \leq 1\frac{1}{2}$. Adding (2) for an arbitrary edge $ab \in E$ and $1 \leq i \leq H$ gives

$$\sum_{i=1}^H w_i \geq \sum_{i=1}^H x_{ai} + \sum_{i=1}^H x_{bi}.$$

From (1) it follows that $\sum_{i=1}^H x_{ai} = \sum_{i=1}^H x_{bi} = 1$, which implies that $\sum_{i=1}^H w_i \geq 2$. Therefore, we have $\nu(\text{ASS}) \geq 2$, which is strictly larger than $\nu(\text{POP}) \leq 1\frac{1}{2}$. So ASS is strictly stronger than POP. ◀

► **Lemma 8.** *The corresponding pure and hybrid POP models are equally strong, i.e.:*

$$\text{POP} = \text{POPH}, \quad (45)$$

$$\text{POP1} = \text{POPH1}, \quad (46)$$

$$\text{POP2} = \text{POPH2}. \quad (47)$$

Proof. Using equality $x_{v,i} = 1 - (l_{v,i} + g_{i,v})$ (constraint (6)) in inequality $x_{u,i} + x_{v,i} \leq 1$ (constraint (24)) of POPH, transforms it to POP, thus $\text{POP} = \text{POPH}$. Using equality $x_{v,1} = 1 - g_{1,v}$ (constraint (28)) in inequality $x_{u,1} + x_{v,1} \leq g_{1,q}$ (constraint (25)) and setting the equality $x_{v,i} = g_{i-1,v} - g_{i,v}$ (constraint (29)) in inequality $x_{u,i} + x_{v,i} \leq g_{i-1,q}$ (constraint (26)) gives (15) and (16), respectively. In this way, one can transform POPH1 to POP1 and POPH2 to POP2. \blacktriangleleft

The following theorem summarizes the polyhedral results, shown in Lemmas 5–8.

► **Theorem 9.** *The following strength-relationships hold:*

$$\begin{array}{ccccc} \text{POP2} & \succ & \text{POP1} & \succ & \text{ASS} & \succ & \text{POP} \\ \parallel & & \parallel & & & & \parallel \\ \text{POPH2} & \succ & \text{POPH1} & & & \succ & \text{POPH}. \end{array}$$

5 Computational Results

As previously analyzed, we expect that the explicit ILP models for the vertex coloring problem such as the assignment and partial-ordering based models are best suited for sparse graphs, whereas the models relying on independent sets are beneficial for dense graphs. In our computational experiments we are interested in answering the following questions:

- (Q1): How do the strengthened partial-ordering based models compare to other explicit coloring models such as the assignment model?
- (Q2): Does one of the strengthened pure and hybrid partial-ordering based models dominate the other?
- (Q3): How do the strengthened models compare to the sophisticated state-of-the-art algorithms relying on independent sets?

5.1 Implementation

We have implemented the assignment and the strongest pure and hybrid partial-ordering based models POP2 and POPH2 using the Gurobi-python API. Our implementation involves the following preprocessings, which are widely used in the literature [14, 15, 18, 22, 23, 26, 27]:

- (a) A vertex u is *dominated* by vertex v , $v \neq u$, if the neighborhood of u is a subset of the neighborhood of v . In this case, the vertex u can be deleted, the remaining graph can be colored, and at the end u can get the color of v .
- (b) To reduce the number of variables we are interested in getting a small upper bound H for the number of needed colors.
- (c) One can fix more variables in the assignment and POP models when precoloring a clique Q with $\max(|Q|H + |\delta(Q)|)$, where $\delta(Q) := \{(u, v) \in E : |\{u, v\} \cap Q| = 1\}$ (see [18]).
- (d) Since any clique represents a valid lower bound for the VCP, in the case of equal lower and upper bounds the optimal value has been found, hence no ILP needs to be solved.

The preprocessing is done using heuristics from the python library **networkx**. The special vertex q is chosen arbitrarily from the clique Q found in the preprocessing, and the remaining vertices in Q are precolored with colors $1, \dots, |Q| - 1$. Moreover, our implementations involve the branching priority option of the Gurobi solver; the higher the degree of a vertex, the higher the branching priority of the associated variables.

Comparison	POP2	POPH2	ASS	HCS[16]	MMT[22]	van Hoeve[34]
DIMACS subset (size)	\mathcal{D}_{our} (116)	\mathcal{D}_{our} (116)	\mathcal{D}_{our} (116)	\mathcal{D}_{our} (116)	\mathcal{D}_{MMT} (115)	\mathcal{D}_{vH} (137)
Machine (CPU)	M_{our} (2.6GHz)	M_{our} (2.6GHz)	M_{our} (2.6GHz)	M_{our} (2.6GHz)	M_{MMT} (2.4GHz)	M_{vH} (2.33GHz)
#solved	74/116 (3h)	84/116 (3h)	81/116 (3h)	62/116 (3h)	70/115 (10h)	50/137 (1h)
#solved/$\mathcal{D}_{\text{our}} \cap \mathcal{D}_{\text{MMT}}$	66/103 (3h)	74/103 (3h)	71/103 (3h)	50/103 (3h)	68/103 (10h)	
#solved/$\mathcal{D}_{\text{our}} \cap \mathcal{D}_{\text{vH}}$ (1h)	74/116 ($\frac{2.33}{2.6}$ h)	82/116 ($\frac{2.33}{2.6}$ h)	80/116 ($\frac{2.33}{2.6}$ h)	62/116 ($\frac{2.33}{2.6}$ h)		49/116 (1h)
average runtime	71.1 sec	261.2 sec	168.7 sec	92.1 sec	434.2 sec	74.7 sec

■ **Table 1** Experimental results for state-of-the-art ILP models for the DIMACS [33] benchmark set $\mathcal{D} = \mathcal{D}_{\text{vH}}$ and subsets \mathcal{D}_{our} and \mathcal{D}_{MMT}

5.2 Test setup and benchmark set of graphs

To solve the implemented models, we used Gurobi 6.5 single-threadedly on the machine with Intel E5-2640@2.60GHz running Ubuntu 18.04. For computational comparisons we also compiled the code of the Held, Cook, and Sewell [16] model on a same machine and with the same Gurobi version. The **dfmax** benchmark [10], which is used in the DIMACS challenge to compare the results obtained with different machines, needs 5.0s for **r500.5** on our machine. We performed our evaluations on a subset of the DIMACS [33] benchmark set. From 137 DIMACS graphs we have chosen all instances that have at most 100 000 edges. The largest one, namely **4-FullIns_5**, of the chosen 116 instances has 4 146 vertices and 77 305 edges. We have set a time limit of three hours.

5.3 Experimental evaluation

Table 1 summarizes some experimental results on the DIMACS instances. Column 1 shows the subjects of the comparison, while the remaining column 2–7 display the associated results of the models POP2, POPH2, ASS, Held, Cook, and Sewell [16], referred to as HCS, Malaguti, Monaci, and Toth [22], referred to as MMT, and van Hoeve [34]. While Columns 2–5 show the results of our computations, the last two columns are taken from [22, 34]. Let \mathcal{D} denote the DIMACS [33] benchmark set and let \mathcal{D}_{our} , \mathcal{D}_{MMT} and \mathcal{D}_{vH} denote the subsets of \mathcal{D} used in our experiments, in Malaguti, Monaci, and Toth [22] and in van Hoeve [34], respectively. \mathcal{D}_{our} and \mathcal{D}_{MMT} contain 116 and 115 instances of \mathcal{D} , respectively, while \mathcal{D}_{vH} encloses the whole \mathcal{D} . The intersection of $\mathcal{D}_{\text{our}} \cap \mathcal{D}_{\text{MMT}}$ contains 103 common instances. As $\mathcal{D}_{\text{vH}} = \mathcal{D}$, we have $\mathcal{D}_{\text{our}} \cap \mathcal{D}_{\text{vH}} = \mathcal{D}_{\text{our}}$.

The first two rows show the instances and machines used in the experiments. The next three rows display the number of solved instances by the algorithms. The items in these rows have the form “ n/N (t)”, which shows the number n of solved instances out of N instances within the time limit t . Row “#solved” shows the total number of solved instances by these six models. We can see that the model POPH2 has solved the largest number of instances, namely 84 out of 116 instances within the time limit of 3 hours, to provable optimality.

Figure 1 visualizes some details about this row. We partitioned the 137 DIMACS instances into ten classes $(0, 0.1], \dots, (0.9, 1]$ according to their densities $\frac{2|E|}{|V|(|V|-1)}$. These classes contain 61, 20, 19, 5, 13, 8, 1, 1, 3, 6 instances, respectively. The figure provides the following information for each density class: The wide box shows the total number of instances in the class. For each ILP model, the corresponding filled bar shows the number of instances solved by that model, while the unfilled bar shows the number of instances that were evaluated but could not be solved by the model. For example in the first class there are 61 instances. We evaluated the models POP2, POPH2, ASS and HCS using 53 out of the 61 instances, where the models solved 37, 43, 40, 22, respectively. Malaguti, Monaci, and Toth [22] and van Hoeve [34] evaluated 56 and 61 out of the 61 instances and solved 29 and

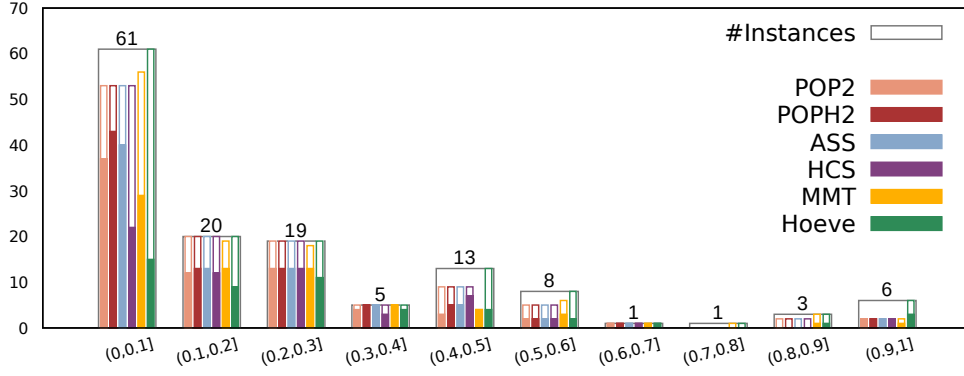


Figure 1 Number of solved DIMACS instances depending on graph density $\frac{2|E|}{|V|(|V|-1)}$ (The density-groups have 61, 20, 19, 5, 13, 8, 1, 1, 3, 6 instances, respectively, and 137 in total.)

15 instances, respectively. We can see that most DIMACS instances are sparse graphs; the first density class, in which POPH2 dominates all other tested models, includes about half of the instances.

Row “#solved/ $\mathcal{D}_{\text{our}} \cap \mathcal{D}_{\text{MMT}}$ ” of Table 1 compares, our experimental results with the results reported by Malaguti, Monaci, and Toth [22] based on the 103 common DIMACS instances. Also here we can see that the model POPH2 has solved the largest number of instances, namely 74. The last row “#solved/ $\mathcal{D}_{\text{our}} \cap \mathcal{D}_{\text{vH}}(1\text{h})$ ” compares, based on the 116 common DIMACS instances, our experimental results with the results reported by van Hoeve [34]. For a fair comparison, it is interesting to see the number of instances solved for each algorithm at similar computing times. To this end, this row shows the number of instances solved for each algorithm at the computing time that roughly corresponds to 1 hour of the machine used in [34]. For example the computing time $\frac{2.33}{2.6}$ hours in our machine roughly corresponds to 1 hour of the $\frac{2.33\text{GHz}}{2.6\text{GHz}}$ times slower machine used in [34]. Also here we can see that the model POPH2 has solved the largest number of instances, namely 82 out of the 116 instances. Finally, the last row shows for each model the average running times spent for the solved instances.

Answering our questions from the beginning, we can state the following:

- (Q1): Our computational study shows that the strengthened hybrid model POPH2 outperforms the assignment formulation ASS on the DIMACS benchmark set, i.e., it solves more DIMACS [33] instances than ASS. This is not true for the pure model POP2.
- (Q2): Although POP2 and POPH2 are equally strong by Theorem 9, the latter solves more instances than the former. The explanation lies in the fact described in Remark 1, which implies that the constraint matrix of the hybrid model becomes sparser than that of the pure model for graphs with $\frac{|E|}{|V|} \geq 1.5$, which is the case for all considered 116 instances.
- (Q3): Our computational results and the studies reported in the literature (also see Table 1) show that the strengthened models POP2 and POPH2 dominate the sophisticated state-of-the-art algorithms [16, 22, 34] on the sparse DIMACS [33] instances with density $\frac{2|E|}{|V|(|V|-1)} \leq 0.1$ (Figure 1). Moreover, a closer look at the single instances (Table 2 in Appendix) shows that the hybrid model POPH2 is the only model, which can solve all five DIMACS GPIA graphs that originated from the estimation of the sparse Jacobian matrix problem [8]. To our knowledge, POPH2 is the first one that can solve the open instance abb313GPIA.

References

- 1 Daniel Brélaz. New methods to color the vertices of a graph. *Commun. ACM*, 22:251–256, 1979.
- 2 J. R. Brown. Chromatic scheduling and the chromatic number problem. *Management Science*, 19(4-part-1):456–463, 1972.
- 3 Jesper Makhholm Byskov. *Chromatic Number in Time $O(2.4023^n)$: Using Maximal Independent Sets*. BRICS, 2002.
- 4 M. B. Campêlo, R. C. Corrêa, and Y. Frota. Cliques, holes and the vertex coloring polytope. *Inf. Process. Lett.*, 89(4):159–164, 2004. doi:10.1016/j.ipl.2003.11.005.
- 5 Manoel B. Campêlo, Victor A. Campos, and Ricardo C. Corrêa. On the asymmetric representatives formulation for the vertex coloring problem. *Discrete Applied Mathematics*, 156(7):1097–1111, 2008.
- 6 V. Campos, R. C. Corrêa, D. Delle Donne, J. Marengo, and A. Wagler. Polyhedral studies of vertex coloring problems: The asymmetric representatives formulation. *ArXiv e-prints*, August 2015. arXiv:1509.02485.
- 7 N. Christofides. An algorithm for the chromatic number of a graph. *The Computer Journal*, 14(1):38–39, 01 1971. URL: <https://doi.org/10.1093/comjnl/14.1.38>, arXiv: <https://academic.oup.com/comjnl/article-pdf/14/1/38/1019738/140038.pdf>, doi:10.1093/comjnl/14.1.38.
- 8 Thomas F. Coleman and Jorge J. Moré. Estimation of sparse jacobian matrices and graph coloring problems. *SIAM Journal on Numerical Analysis*, 20(1):187–209, 1983. URL: <http://www.jstor.org/stable/2157179>.
- 9 D. G. Corneil and B. Graham. An algorithm for determining the chromatic number of a graph. *SIAM Journal on Computing*, 2(4):311–318, 1973. URL: <https://doi.org/10.1137/0202026>, arXiv:<https://doi.org/10.1137/0202026>, doi:10.1137/0202026.
- 10 Benchmarking machines and testing solutions, 2002. URL: <http://mat.gsia.cmu.edu/COLOR02/BENCHMARK/benchmark.tar>.
- 11 D. Eppstein. Small maximal independent sets and faster exact graph coloring. *Journal of Graph Algorithms and Applications*, 7(2):131–140, 2003.
- 12 Michael R. Garey and David S. Johnson. *Computers and Intractability: A Guide to the Theory of NP-Completeness*. W. H. Freeman & Co., 1979.
- 13 Sven Gedicke, Adalat Jabrayilov, Benjamin Niedermann, Petra Mutzel, and Jan-Henrik Haunert. Point feature label placement for multi-page maps on small-screen devices. *Computers & Graphics*, 2021. URL: <https://www.sciencedirect.com/science/article/pii/S0097849321001564>, doi:<https://doi.org/10.1016/j.cag.2021.07.019>.
- 14 S. Gualandi and F. Malucelli. Exact solution of graph coloring problems via constraint programming and column generation. *INFORMS J. on Computing*, 24(1):81–100, 2012.
- 15 P. Hansen, M. Labbé, and D. Schindl. Set covering and packing formulations of graph coloring: Algorithms and first polyhedral results. *Discrete Optimization*, 6(2):135 – 147, 2009.
- 16 S. Held, W. Cook, and E.C. Sewell. Maximum-weight stable sets and safe lower bounds for graph coloring. *Mathematical Programming Computation*, 4(4):363–381, 2012.
- 17 Thore Husfeldt. *Graph colouring algorithms*, pages 277–303. Cambridge University Press, United Kingdom, 2015.
- 18 A. Jabrayilov and P. Mutzel. New integer linear programming models for the vertex coloring problem. In *Latin American Theoretical Informatics Symposium LATIN 2018*, volume 10807 of *LNCs*, pages 640–652. Springer, 2018.
- 19 E. Lawler. A note on the complexity of the chromatic number problem. *Inf. Process. Lett.*, 5:66–67, 1976.
- 20 R. M. R. Lewis. Guide to graph colouring: Algorithms and applications. *Guide to Graph Colouring*, 2016.
- 21 A. M. D. Lima and R. Carmo. Exact algorithms for the graph coloring problem. *RITA*, 25:57–73, 2018.

- 22 E. Malaguti, M. Monaci, and P. Toth. An exact approach for the vertex coloring problem. *Discrete Optimization*, 8(2):174–190, 2011.
- 23 E. Malaguti and P. Toth. A survey on vertex coloring problems. *International Transactions in Operational Research*, 17:1–34, 2010.
- 24 Colin McDiarmid. Determining the chromatic number of a graph. *SIAM J. Comput.*, 8:1–14, 1979.
- 25 A. Mehrotra and M. Trick. A column generation approach for graph coloring. *INFORMS Journal On Computing*, 8(4):344–354, 1996.
- 26 I. Méndez-Díaz and P. Zabala. A branch-and-cut algorithm for graph coloring. *Discrete Applied Mathematics*, 154(5):826–847, 2006.
- 27 I. Méndez-Díaz and P. Zabala. A cutting plane algorithm for graph coloring. *Discrete Applied Mathematics*, 156(2):159 – 179, 2008.
- 28 Emanuel Florentin Olariu and Cristian Frasinaru. Improving lower bounds for equitable chromatic number. *CoRR*, abs/2106.03409, 2021. URL: <https://arxiv.org/abs/2106.03409>, arXiv:2106.03409.
- 29 Tobias Polzin and Siavash Vahdati-Daneshmand. *Approaches to the Steiner Problem in Networks*, pages 81–103. Springer Berlin Heidelberg, Berlin, Heidelberg, 2009. URL: https://doi.org/10.1007/978-3-642-02094-0_5, doi:10.1007/978-3-642-02094-0_5.
- 30 Hazhar Rahmani and J. O’Kane. Integer linear programming formulations of the filter partitioning minimization problem. *Journal of Combinatorial Optimization*, 40:431–453, 2020.
- 31 P. San Segundo. A new DSATUR-based algorithm for exact vertex coloring. *Computers & Operations Research*, 39(7):1724 – 1733, 2012.
- 32 E. Sewell. An improved algorithm for exact graph coloring. In *Cliques, Coloring, and Satisfiability*, 1993.
- 33 M. Trick. DIMACS graph coloring instances, 2002. URL: <http://mat.gsia.cmu.edu/COLOR02/>.
- 34 Willem-Jan van Hoeve. Graph coloring with decision diagrams. *Mathematical Programming*, 192:631–674, 2022. doi:10.1007/s10107-021-01662-x.
- 35 Alexander Aleksandrovich Zykov. On some properties of linear complexes. *Matematicheskii sbornik*, 66(2):163–188, 1949.

A Computational Results

Table 2 shows the detailed results for the 116 DIMACS [33] instances that we have used in our computational evaluations. Recall that we have considered only the instances with up to 100 000 edges.

Columns 1-3 show the instance names and sizes. Columns 4-15 display the lower and upper bounds as well as the running times of the models POP2, POPH2, ASS, and HCS [16] that we have obtained within a time limit of three hours in our computations. The times are provided in seconds.

Columns 16-18 are taken from the literature [22] and show the results of sophisticated state-of-the-art algorithm suggested by Malaguti, Monaci, and Toth [22]. These results have been obtained within a time limit of ten hours. The columns contain the character “-” if the associated instances were not considered in [22].

The last three columns are taken from [34] and show the results of the sophisticated algorithm suggested by van Hoeve [34]. Note that these results have been obtained within a time limit of one hour.

Instance	POP2		POPH2		ASS		HCS [16]		MMT [22]		v.Hoeve[34]	
	lb	ub	lb	ub	lb	ub	lb	ub	lb	ub	lb	ub
1-Fullus_3	30	100	4.0	4.0	0.0	0.0	4.0	4.0	-	-	4	4
1-Fullus_4	93	593	5.0	5.0	0.0	0.0	4.0	5.0	4	5	4	5
1-Fullus_5	282	3247	6.0	6.0	0.9	0.7	4.0	6.0	4	6	4	6
1-Insertions_4	67	232	5.0	5.0	33.3	8.7	4.0	5.0	3	5	3	5
1-Insertions_5	202	1227	4.0	6.0	timeout	4.0	4.0	6.0	3	6	3	6
1-Insertions_6	607	6337	4.0	7.0	timeout	4.0	4.0	7.0	3	7	3	7
2-Fullus_3	52	201	5.0	5.0	0.0	0.0	5.0	5.0	5	5	5	5
2-Fullus_4	212	1621	6.0	6.0	0.0	0.0	5.0	6.0	5	6	5	6
2-Fullus_5	852	12201	7.0	7.0	1.8	1.8	5.0	7.0	5	7	4	7
2-Insertions_3	37	72	4.0	4.0	0.1	0.1	4.0	4.0	-	-	3	4
2-Insertions_4	149	541	4.0	5.0	timeout	4.0	4.0	5.0	3	5	3	5
2-Insertions_5	597	3936	4.0	6.0	timeout	4.0	4.0	6.0	3	6	3	6
3-Fullus_3	80	346	6.0	6.0	0.0	0.0	6.0	6.0	6	6	6	6
3-Fullus_4	405	3524	7.0	7.0	0.0	0.0	6.0	7.0	6	7	5	7
3-Fullus_5	2030	33751	8.0	8.0	3.2	3.2	6.0	8.0	6	8	5	8
3-Insertions_3	56	110	4.0	4.0	0.9	0.9	4.0	4.0	3	4	3	4
3-Insertions_4	281	1046	4.0	5.0	timeout	4.0	3.0	5.0	3	5	3	5
3-Insertions_5	1406	9695	3.0	6.0	timeout	3.0	3.0	6.0	2	6	3	6
4-Fullus_3	114	541	7.0	7.0	0.0	0.0	7.0	7.0	7	7	7	7
4-Fullus_4	690	6650	8.0	8.0	0.0	0.0	8.0	8.0	7	8	7	8
4-Fullus_5	4146	77305	9.0	9.0	7.7	7.7	9.0	9.0	7	9	7	9
4-Insertions_3	79	156	4.0	4.0	20.3	20.3	4.0	4.0	3	4	3	4
4-Insertions_4	475	1795	3.0	5.0	timeout	3.0	3.0	5.0	3	5	3	5
5-Fullus_3	154	792	8.0	8.0	0.0	0.0	8.0	8.0	8	8	8	8
5-Fullus_4	1085	11395	9.0	9.0	0.1	0.1	9.0	9.0	8	9	8	9
5-Fullus_5	1555	53356	8.0	10.0	timeout	8.0	8.0	11.0	8	10	8	10
abb313GPIA	138	493	11	11	0	0	11	11	11	11	11	11
ama	662	4181	4.0	4.0	15.5	15.5	4.0	4.0	4	4	4	4
ash331GPIA	1216	7844	4.0	4.0	1902.7	1902.7	4.0	4.0	4	4	3	5
ash608GPIA	1916	12506	4.0	4.0	342.7	342.7	4.0	4.0	3	4	3	5
ash958GPIA	87	406	11	11	0	0	11	11	11	11	11	11
david	1000	49629	6.0	29.0	timeout	6.0	6.0	29.0	-∞	-∞	6	26
DSJ/C1000.1	125	736	5.0	5.0	3.1	3.1	5.0	5.0	5	5	5	6
DSJ/C125.1	125	3891	11.0	20.0	timeout	13.0	13.0	19.0	17	17	14	22
DSJ/C125.5	125	6961	35.0	47.0	timeout	40.0	40.0	44.0	44	44	44	44
DSJ/C250.1	250	3218	5.0	9.0	timeout	5.0	5.0	9.0	6	8	5	10
DSJ/C250.5	250	15668	12.0	41.0	timeout	14.0	14.0	38.0	20	28	16	36
DSJ/C250.9	250	27897	40.0	+∞	timeout	42.0	42.0	90.0	71	72	71	74
DSJ/C500.1	500	12458	5.0	17.0	timeout	6.0	6.0	18.0	5	12	5	16
DSJ/C500.5	500	62624	13.0	70.0	timeout	13.0	13.0	+∞	16	48	18	68

Table 2 Results of the six models for the DIMACS [33] instances with up to 100000 edges

Instance	V	E	POP2			POPH2			ASS			HCS [16]			MMT [22]			v.Hoeve[34]		
			lb	ub	time[s]	lb	ub	time[s]	lb	ub	time[s]	lb	ub	time[s]	lb	ub	time[s]	lb	ub	time[s]
DSJR500.1	500	3555	12.0	12.0	2.7	12.0	12.0	0.7	12.0	12.0	0.5	12	12	1165.9	12	12	35.3	12	12	0.03
DSJR500.5	500	58862	115.0	135.0	timeout	120.0	+∞	timeout	115.0	128.0	timeout	122	132	timeout	122	122	342.2	112	126	timeout
flat300_20_0	300	21375	11.0	+∞	timeout	12.0	+∞	timeout	12.0	43.0	timeout	20	20	10.2	-	-	-	16	42	timeout
flat300_26_0	300	21633	11.0	45.0	timeout	13.0	+∞	timeout	12.0	43.0	timeout	26	26	24.3	-	-	-	16	43	timeout
flat300_28_0	300	21695	12.0	45.0	timeout	13.0	+∞	timeout	14.0	43.0	timeout	28	41	timeout	-	-	-	16	44	timeout
fpsol2.1.1	269	11654	65	65	0	65	65	0	65	65	0	65	65	0.6	65	65	10.6	65	65	10.33
fpsol2.1.2	363	8691	30	30	0	30	30	0	30	30	0	30	30	0.4	30	30	11.2	30	30	0.21
fpsol2.1.3	363	8688	30	30	0	30	30	0	30	30	0	30	30	0.3	30	30	10.0	30	30	0.25
games120	120	638	9	9	0	9	9	0	9	9	0	9	9	0.0	9	9	0.2	9	9	92.74
homer	556	1629	13	13	0	13	13	0	13	13	0	13	13	0.1	-	-	-	10	13	timeout
huck	74	301	11	11	0	11	11	0	11	11	0	11	11	0.0	11	11	0.2	11	11	0.23
inithx.1	519	18707	54	54	0	54	54	0	54	54	0	54	54	2.1	54	54	21.0	54	54	3.17
inithx.2	558	13979	31	31	0	31	31	0	31	31	0	31	31	0.7	31	31	9.2	31	31	121.09
inithx.3	559	13969	31	31	0	31	31	0	31	31	0	31	31	0.8	31	31	9.9	31	31	163.70
jean	77	254	10	10	0	10	10	0	10	10	0	10	10	0.0	10	10	0.2	10	10	0.01
le450_15a	450	8168	15.0	16.0	timeout	15.0	15.0	1032.0	15.0	15.0	1157.2	15	17	timeout	15	15	0.4	15	18	timeout
le450_15b	450	8169	15.0	15.0	1088.2	15.0	15.0	1384.6	15.0	15.0	1261.2	15	17	timeout	15	15	0.2	15	17	timeout
le450_15c	450	16680	15.0	23.0	timeout	15.0	+∞	timeout	15.0	27.0	timeout	15	15	349.7	15	15	3.1	15	25	timeout
le450_15d	450	16750	15.0	23.0	timeout	15.0	+∞	timeout	15.0	27.0	timeout	15	15	383.3	15	15	3.8	15	25	timeout
le450_25a	450	8260	25	25	0	25	25	0	25	25	0	25	25	2.7	25	25	0.1	25	25	0.17
le450_25b	450	8263	25	25	0	25	25	0	25	25	0	25	25	2.3	25	25	0.1	25	25	0.14
le450_25c	450	17343	25.0	27.0	timeout	25.0	27.0	timeout	25.0	27.0	timeout	25	28	timeout	25	25	1356.6	25	29	timeout
le450_25d	450	17425	25.0	27.0	timeout	25.0	27.0	timeout	25.0	28.0	timeout	25	29	timeout	25	25	66.6	25	28	timeout
le450_5a	450	5714	5.0	9.0	timeout	5.0	5.0	103.9	5.0	5.0	44.7	5	6	timeout	5	5	0.3	5	10	timeout
le450_5b	450	5734	5.0	7.0	timeout	5.0	5.0	89.5	5.0	5.0	214.6	5	5	760.8	5	5	0.2	5	9	timeout
le450_5c	450	9803	5.0	5.0	622.4	5.0	5.0	24.3	5.0	5.0	23.5	5	5	368.6	5	5	0.1	5	8	timeout
le450_5d	450	9757	5.0	5.0	760.9	5.0	5.0	24.6	5.0	5.0	29.3	5	6	timeout	5	5	0.2	5	5	0.03
miles1000	128	3216	42.0	42.0	6.7	42.0	42.0	1.2	42.0	42.0	0.5	42	42	0.1	42	42	0.2	42	42	1.87
miles1500	128	5198	73	73	0	73	73	0	73	73	0	73	73	0.2	73	73	0.1	73	73	1.10
miles250	125	387	8	8	0	8	8	0	8	8	0	8	8	0.0	8	8	5.0	8	8	0.01
miles500	128	1170	20	20	0	20	20	0	20	20	0	20	20	0.0	20	20	3.7	20	20	0.04
miles750	128	2113	31.0	31.0	1.0	31.0	31.0	0.6	31.0	31.0	0.3	31	31	0.1	31	31	0.2	31	31	0.12
mug100_1	100	166	4.0	4.0	0.1	4.0	4.0	0.1	4.0	4.0	0.1	4	4	1.0	4	4	14.4	3	4	timeout
mug100_25	100	166	4.0	4.0	0.2	4.0	4.0	0.2	4.0	4.0	0.2	4	4	0.9	4	4	12.0	3	4	timeout
mug88_1	88	146	4.0	4.0	0.1	4.0	4.0	0.1	4.0	4.0	0.1	4	4	0.6	4	4	9.6	3	4	timeout
mug88_25	88	146	4.0	4.0	0.3	4.0	4.0	0.1	4.0	4.0	0.1	4	4	0.6	4	4	10.6	3	4	timeout
musoli.1	138	3925	49	49	0	49	49	0	49	49	0	49	49	0.2	49	49	0.2	49	49	0.40
musoli.2	173	3885	31	31	0	31	31	0	31	31	0	31	31	0.1	31	31	4.7	31	31	0.19
musoli.3	174	3916	31	31	0	31	31	0	31	31	0	31	31	0.1	31	31	0.2	31	31	0.19
musoli.4	175	3946	31	31	0	31	31	0	31	31	0	31	31	0.1	31	31	0.2	31	31	0.19

Table 2 (continued)

Instance	V	E	POP2			POP42			ASS			HCS [16]			MMT [22]			v.Hoeve[34]		
			lb	ub	time[s]	lb	ub	time[s]	lb	ub	time[s]	lb	ub	time[s]	lb	ub	time[s]	lb	ub	time[s]
multisli.5	176	3973	31	31	0	31	31	0	31	31	0	31	31	0.1	31	31	6.0	31	31	0.19
myciel3	11	20	4.0	4.0	0.0	4.0	4.0	0.0	4.0	4.0	0.0	4	4	0.0	4	4	0	4	4	0.04
myciel4	23	71	5.0	5.0	0.1	5.0	5.0	0.1	5.0	5.0	0.1	5	5	8.1	5	5	4	5	5	7.03
myciel5	47	236	6.0	6.0	5.2	6.0	6.0	2.5	6.0	6.0	3.5	5	6	timeout	-∞	+	timeout	5	6	timeout
myciel6	95	755	6.0	7.0	timeout	7.0	7.0	2286.0	7.0	7.0	7730.0	5	7	timeout	4	7	timeout	4	7	timeout
myciel7	191	2360	5.0	8.0	timeout	5.0	8.0	timeout	6.0	8.0	timeout	5	8	timeout	5	8	timeout	4	8	timeout
qg.order30	900	26100	30.0	+∞	timeout	30.0	30.0	70.1	30.0	30.0	55.9	30	32	timeout	30	30	0.2	30	32	timeout
qg.order40	1600	62400	40.0	55.0	timeout	40.0	40.0	4318.9	-∞	64.0	timeout	40	42	timeout	40	40	2.9	40	45	timeout
queen10_10	100	1470	10.0	12.0	timeout	10.0	11.0	timeout	10.0	11.0	timeout	11	14	timeout	11	11	686.9	10	14	timeout
queen11_11	121	1980	11.0	13.0	timeout	11.0	13.0	timeout	11.0	13.0	timeout	11	11	61.9	11	11	1865.7	10	15	timeout
queen12_12	144	2596	12.0	14.0	timeout	12.0	14.0	timeout	12.0	14.0	timeout	12	16	timeout	12	13	timeout	10	16	timeout
queen13_13	169	3328	13.0	15.0	timeout	13.0	15.0	timeout	13.0	15.0	timeout	13	17	timeout	13	14	timeout	10	17	timeout
queen14_14	196	4186	14.0	17.0	timeout	14.0	17.0	timeout	14.0	16.0	timeout	14	19	timeout	14	15	timeout	10	19	timeout
queen15_15	225	5180	15.0	18.0	timeout	15.0	18.0	timeout	15.0	18.0	timeout	15	20	timeout	15	16	timeout	10	21	timeout
queen16_16	256	6320	16.0	19.0	timeout	16.0	19.0	timeout	16.0	19.0	timeout	16	21	timeout	16	17	timeout	10	22	timeout
queen5_5	25	160	5.0	5.0	0.0	5.0	5.0	0.0	5.0	5.0	0.0	5	5	0.0	5	5	0.2	5	5	0.01
queen6_6	36	290	7.0	7.0	0.4	7.0	7.0	0.2	7.0	7.0	0.2	7	7	5.0	7	7	3	7	7	2.35
queen7_7	49	476	7.0	7.0	4.4	7.0	7.0	0.3	7.0	7.0	0.3	7	7	0.0	7	7	0.2	7	7	2.77
queen8_12	96	1368	12.0	12.0	8.1	12.0	12.0	1.9	12.0	12.0	1.1	12	12	9.6	12	12	0.2	9	12	timeout
queen8_8	64	728	9.0	9.0	195.7	9.0	9.0	14.2	9.0	9.0	38.9	9	11	timeout	9	9	3.6	9	9	310.31
queen9_9	81	1056	9.0	10.0	timeout	10.0	10.0	1369.9	10.0	10.0	1621.2	10	12	timeout	10	10	36.6	10	12	timeout
r1000.1	1000	14378	20.0	20.0	126.3	20.0	20.0	19.5	20.0	20.0	17.9	20	20	1.2	-	-	-	20	20	0.20
r125.1c	125	7501	46	46	0	46	46	0	46	46	0	46	46	0.0	-	-	-	46	46	2.08
r125.1	122	209	5	5	0	5	5	0	5	5	0	5	5	0.0	-	-	-	5	5	0.02
r125.5	125	3838	34.0	36.0	timeout	36.0	36.0	3.2	36.0	36.0	3.2	36	36	72.9	-	-	-	36	36	212.90
r250.1c	250	30227	64	64	0	64	64	0	64	64	0	64	64	0.2	-	-	-	64	64	31.19
r250.1	250	867	8	8	0	8	8	0	8	8	0	8	8	0.0	-	-	-	8	8	7.32
r250.5	250	14849	65.0	66.0	timeout	65.0	65.0	17.7	65.0	65.0	7.3	65	65	2046.6	-	-	-	65	67	timeout
school1	385	19095	14.0	14.0	36.9	14.0	14.0	39.6	14.0	14.0	36.2	14	14	88.4	14	14	0.4	14	14	1.67
school1_nsh	352	14612	14.0	14.0	35.7	14.0	14.0	36.1	14.0	14.0	35.2	14	14	82.1	14	14	17.0	14	14	15.59
wap05a	905	43081	50	50	0	50	50	0	50	50	0	50	50	7.9	50	50	293.2	50	50	15.80
wap06a	947	43571	40.0	+∞	timeout	40.0	+∞	timeout	40.0	+∞	timeout	40	44	timeout	40	40	175.0	40	43	timeout
will199GPIA	701	6772	7.0	7.0	9.0	7.0	7.0	2.5	7.0	7.0	5.5	7	7	2.3	7	7	80.7	6	7	timeout
zeroin.1	126	4100	49	49	0	49	49	0	49	49	0	49	49	0.2	49	49	3.8	49	49	0.32
zeroin.12	157	3541	30	30	0	30	30	0	30	30	0	30	30	0.1	30	30	4.4	30	30	0.17
zeroin.13	157	3540	30	30	0	30	30	0	30	30	0	30	30	0.0	30	30	4.5	30	30	0.20

Table 2 (continued)